Computational investigation of positron scattering from C_{60}

F. A. Gianturco
Department of Chemistry, The University of Rome, Cittá Universitaria, 00185 Rome, Italy

Robert R. Lucchese
Department of Chemistry, Texas A&M University, College Station, Texas 77843-3255

(Received 5 May 1999)

The low-energy (0–6-eV) behavior of positrons scattering from gaseous C_{60} molecules is examined through a computational study which employs a nonempirical modeling of all the relevant interaction forces (static, correlation, and polarization potentials). There is uncertainty concerning the most appropriate correlation-polarization potential to use in the study of positron-molecule scattering. Here we have considered two such potentials which are representative of the potentials which have been proposed for this purpose. The coupled quantum scattering equations are solved in the body-fixed frame of reference, and the fixed-nuclei approximation is used to decouple the nuclear motion during the collision. The elastic integral cross sections without positronium formation exhibit strong one-particle resonances in the very-low-energy region up to ~4 eV. The low-angular-momentum scattering components are shown to be the dominant contributions to trapped state wave functions. The existence of resonances in positron scattering from molecules is unusual. In the system studied here there are two types of resonances. First there are angular-momentum barrier resonances with the positron trapped outside of the C_{60} cage. Second, there are resonances of low angular momentum ($l \leqslant 2$) with the positron trapped inside of the C_{60} cage by the repulsive interaction between the positron and the nuclei. The possibility of the experimental observation of these resonances is also discussed. [S1050-2947(99)08511-X]

PACS number(s): 34.85.+x

I. INTRODUCTION

The study of low-energy positron scattering from molecules has a long history related to the interest in positron annihilation in gases and in the slowing down of positrons in several media [1,2]. Due to the additional internal degrees of freedom (e.g., rotational and vibrational inelastic processes), molecules are more efficient than atoms for the slowing down of positrons, particularly in the low-energy regimes [3,4]. Furthermore, the existence of rather important ''reactive'' channels for positron scattering, which are absent in electron scattering, makes the study of the positron-molecule dynamics an intriguing subject at the fundamental level of investigation. Thus, there exists the possibility that positronium (Ps) formation creates molecular ions which are obtained rather ''gently,'' and therefore can be experimentally observed for longer times than those formed by impact ionization processes. The particle-antiparticle decay channel, whereby pickoff of a bound electron leads to the emission of two γ photons and to cation formation from the molecular target, is also an alternative channel of marked experimental interest [5]. Finally, the possibility of the positron binding to the molecular target, and the consequent formation of a molecular cation, is also a further ''reactive'' channel that has received a great deal of attention, both experimentally and theoretically, albeit escaping observation thus far even for the simplest molecules [6]. The analogy with electron scattering becomes more direct in the case of the positron open-channel resonances, whereby one-particle trapping is thought to occur without much target excitation but rather via potential shape effects, as is the case of the well-known shape resonances of electron-molecule scattering [7].

In the case of electron scattering, in fact, the C_{60} molecule is an ideal candidate for such processes since both its rather large spatial extent and the existence of empty space *inside* the cage of atoms is known to lead easily to the trapping of electrons and to the formation of fairly stable, negative ions of C_{60} [8,9]. It is therefore of interest to see what sort of behavior would be exhibited by positron scattering on the same system, and how it may be seen by the measurements of the corresponding cross sections at low energies. As we are not aware as yet of any experimental result regarding positron scattering from the C_{60} molecule, to our knowledge here we are presenting the first calculations on the positron scattering from fullerene in order to both stimulate the appearance of possible experiments and to put forward some unusual results obtained from calculations that should entice even more the collection of experimental data on this system.

The paper is organized as follows: in Sec. II we briefly outline our theoretical treatment, while Sec. III reports the results of our calculations and presents the behavior of the low-energy elastic cross sections, integral, and differential. Section IV finally summarizes our conclusions, and suggests possible routes to experimental detection.

II. THEORETICAL MODEL

When discussing the quantum dynamics of positron collisions with molecular systems at energies below the threshold for Ps formation, one is required to know the following aspect of the process: (i) the anisotropic charge distribution of the molecular target, and the corresponding static interaction of the target with the impinging positron; (ii) the short- and medium-range descriptions of the electron-positron dynamical correlation, and (iii) the long-range behavior of the target response to the e^+ perturbation, i.e., the polarization poten-

tial. For simplicity we also assume that the nuclear motion is decoupled from the positron dynamics during the scattering process and we thus compute the positron scattering using the fixed-nuclei (FN) approximation.

The above three points, therefore, need to be taken into account before the actual dynamics can be investigated. As in our previous work on positron-molecule scattering [10,11], the actual evaluation of the static interaction, $V_S(\mathbf{r}_p)$, was carried out by expanding the self-consistent-field (SCF) wave function of the C_{60} molecule at its equilibrium geometry (see below for details) around the molecular center of mass (CM) using symmetry-adapted angular functions which transform with the relevant irreducible representation (IR) of the molecular point group, the icosahedral group I_h. The details of the actual procedure we employed will be given in Sec. III. Below the threshold of Ps formation (which is around 1.2 eV in the present case), and above it for the elastic component of the total integral cross sections, one of the most serious questions concerns the clarification of the role played by long-range polarization forces and by short-range dynamical correlation effects. Their balanced combination, in fact, turns out to usually yield final cross sections which are sensitive to the detailed handling of both above contributions, especially at an energy around Ps formation [12].

The more direct approach to the inclusion of positron-electron correlation, usually involves an extensive configuration-interaction expansion of the target electronic wave function over a suitable set of excited electronic configurations and further improvement of the wave function by adding Hylleraas-type functions which can describe the positron wave function within the physical space of the target electronic charge distribution [13]. Such expansions, however, are markedly energy dependent, and usually converge too slowly to be a useful tool for general implementation for complex molecular targets, where truncated expansions need to be very large before they begin to be realistic in describing correlation effects [14,15]. As a consequence, over the years we have developed more tractable global models of such effects which do not depend on empirical parameters but can be easily implemented via a simplified, local representation of the correlation-polarization, $V_{CP}(\mathbf{r}_p)$, interactions [16–18].

To begin with, one should note that the asymptotic form of the above interaction is independent of the sign of the impinging charged particle and, in its simpler spherical form, is given by the well-known second-order perturbation expansion formula in atomic units,

$$V_{CP}(\mathbf{r}_p) = \sum_{l=1}^{\infty} -\frac{\alpha_l}{2r_p^{2l+2}}, \tag{1}$$

where r_p represents now the scalar positron distance from the molecular CM, and α_l are the multipolar static polarizabilities of the molecule, which obviously depend on the nuclear coordinates and on the electronic state of that target. In most cases only the lowest order is kept in the expansion given in Eq. (1), and therefore the target distortion is viewed as chiefly resulting from the induced dipole contribution with the molecular dipole polarizability as its coefficient [15]. The drawback of the above expansion, however, is that it fails to represent correctly the true short-range behavior of the full interaction and does not contain any effect from both static and dynamic correlation contributions [19]. Therefore, a while ago, we proposed [16–18,20], in order to correct for such failures, to use a local density-functional approximation, whereby the dynamic correlation effects that dominate the short-range behavior of the $V_{CP}(\mathbf{r}_p)$ interaction with closed-shell molecular targets can be treated using a density functional theory (DFT) approach within the range of the target electronic density and can be further connected with the asymptotic dipolar form of Eq. (1) in the long-range region.

We therefore describe the full $V_{CP}(\mathbf{r}_p)$ interaction as given by two distinct contributions which are connected at a distance, r_p^c [16]

$$V_{CP}(\mathbf{r}_p) = \begin{cases} V_{corr}^{DFT}(\mathbf{r}_p), & r_p \leqslant r_p^c \\ V_{pol}(\mathbf{r}_p), & r_p > r_p^c. \end{cases} \tag{2}$$

Furthermore, as discussed earlier [16], the short-range correlation contributions in Eq. (2) can be included either by considering the correlation effects on an homogeneous electron gas without reference to the positron projectile, as presented in Ref. [21], or by considering explicitly the positron projectile as an impurity within the homogeneous electron gas [22]. We have explicitly derived both forms of V_{CP}, and discussed their merits for molecular targets in our earlier work. Both models will be employed in the present work. The potential based on the homogeneous electron gas will be that proposed by Perdew and Zunger [23], and will be referred to as the electron correlation potential (ECP), $V_{ECP}(\mathbf{r}_p)$. The form based on the density functional theory for an isolated positron interacting with an electron gas will be referred to as the positron correlation potential (PCP), $V_{PCP}(\mathbf{r}_p)$, and is a modified version of the PCP2 potential proposed by Jain [24] which was derived from the density-functional energy expression of Boronski and Nieminen [22]. We have modified this potential to smoothly cut off the potential as $r_s \to \infty$ by using function

$$V_{corr}(r_s) = \frac{1}{2}\left\{\frac{5.7382}{r_s^2} - \frac{3.5845}{r_s}\right\}, \tag{3}$$

when $r_s \geqslant 4.0$. The total interaction potential is then given as the sum of the static and correlation-polarization potentials to yield

$$V_{tot}(\mathbf{r}_p) = V_S(\mathbf{r}_p) + V_{CP}(\mathbf{r}_p), \tag{4}$$

where V_{CP} is either V_{ECP} or V_{PCP} as discussed above.

The corresponding close-coupling (CC) scattering equations, in the single-center-expansion (SCE) formulation, are given by the expression

$$\left\{\frac{1}{2}\frac{d^2}{dr_p^2} - \frac{l(l+1)}{2r_p^2} + E_{coll}\right\} f_{hl}^{p\mu}(r_p) = \sum_{h'l'} V_{hl,h'l'}^{p\mu}(r_p) f_{h'l'}^{p\mu}(r_p), \tag{5}$$

where E_{coll} is the collision energy, and the positron continuum radial functions $f_{h'l'}^{p\mu}(r_p)$ are the required unknown

quantities originating from the symmetry-adapted SCE form of the wave function of the scattered particle:

$$F_{p\mu}(\mathbf{r}_p)=\sum_{hl} r_p^{-1} f_{hl}^{p\mu}(r_p) X_{hl}^{p\mu}(\hat{r}_p). \tag{6}$$

Here $(p\mu)$ labels the relevant IR, with p describing the IR of the scattered positron and with μ being one of its component and $X_{hl}^{p\mu}(\hat{r}_p)$ are the generalized harmonics. The index h further labels a specific angular basis function for each chosen partial wave contribution l found in the pth IR under consideration. The coupling matrix element on the right-hand side of Eq. (5) is then given by

$$V_{hl,h'l'}^{p\mu}(r_p)=\langle X_{hl}^{p\mu}|V_{\rm tot}(\mathbf{r}_p)|X_{h'l'}^{p\mu}\rangle. \tag{7}$$

The details of the angular products have been described before [25], and will therefore not be repeated here. Suffice it to say that, when using the static plus correlation plus polarization (SCP) interaction within the SCE formulation and the CC dynamical formalism implied by Eq. (5), the formulation and the corresponding coupled-differential equations are solved within the SCP-SCE treatment and finally yield rotationally summed, integral elastic cross sections for each IR contributing to the scattering process. The total cross section is therefore simply given as

$$\sigma_{\rm tot}(E_{\rm coll})=\sum_{p,\mu} \sigma_{p,\mu}^{\rm el}(E_{\rm coll}). \tag{8}$$

The individual K-matrix elements, for each $(p\mu)$, will also provide the total elastic (rotationally summed) differential cross sections (DCS's) that are again summed over all contributing IR at the considered collision energy.

One should mention at this point that the above treatment does not include any contribution from the process of Ps formation. Considering that the ionization potential of C_{60} is around 7.6 eV [25] and that the binding energy of Ps is 6.8 eV, then one sees that the threshold for Ps formation in this system is really at very low energy, i.e., around 1 eV. Despite many experimental attempts for several systems, however, very few accurate measurements of absolute cross sections for this process in atomic and molecular targets have become available to date. The general findings from the more recent experiments are that Ps formation in molecular systems usually peaks around 27–30 eV, while its percentage value just above threshold varies significantly with the type of molecule [26]. In the present case, electronic excitation begins also to contribute from around 4 eV [25], and therefore it does not contribute in the region between 1 and 4 eV, where Ps formation should also be still rather small. Such general considerations should therefore help us to better understand the significance, and the likely detectability, of the features in the integral cross section (ICS) that we will be discussing in Sec. III.

An additional tool that we have used to analyze the scattering process in electron-molecule scattering is the adiabatic static model-exchange correlation polarization potential (ASMECP) [27,28]. To obtain the ASMECP potential, the angular part of Eq. (5) is diagonalized at each radial point r_p. The eigenvalues then are an effective radial adiabatic potential for the electron scattering problem. These adiabatic potentials have been found to be useful in visualizing the structure of the potential, and they can also be used as the basis for solving the scattering problem through a set of coupled radial differential equations similar to Eq. (5) in which the potential is diagonal but in which the radial coupling is not diagonal. In positron-molecule scattering, there is no nonlocal exchange interaction, so that within the local correlation-polarization approximation used here, the full potential used in this study is local hence the adiabatic form of the scattering equation will yield the same scattering states as the form of the scattering equation given in Eq. (5). For the positron-molecule scattering problem, we will refer to the adiabatic static correlation polarization (ASCP) potential as either $V_{\rm ASECP}$ or $V_{\rm ASPCP}$ depending on which form of $V_{\rm CP}$ is being used. The ASCP potential also forms the basis for the analysis of the resonant state in the scattering system. For each resonance, we solve the scattering equations at complex energies to obtain the S matrix. Then poles of the S matrix are located yielding directly the resonance widths and energies. In addition, we can plot the wave function at the complex energy to examine its qualitative features, e.g., the major partial-wave components.

III. RESULTS

In order to start the investigation of possible positron scattering features in the case of C_{60} as a target, we have restricted the study to the ground electronic state and to the equilibrium geometry of C_{60}. The target is represented by a SCF wave function expanded via the 3–21-G basis set as described in the GAUSSIAN 94 suite of codes [29]. With 360 bound electrons we found a SCF total energy of -2259.027868 a. u. The chosen geometry was with C-C bond lengths of 1.450 and 1.391 Å [30]. As discussed before, the description of the scattering process includes the representation of the full, nonspherical nature of the positron interaction with molecular nuclei and electrons and all the calculations were performed using the icosahedral I_h symmetry of the target. One should note the large value of the spherical dipole polarizability of C_{60} which is 558.0 a.u.^{3} [31], an aspect of the problem which will be of paramount importance in our discussion below.

The $V_{\rm CP}$ potentials (both $V_{\rm ECP}$ and $V_{\rm PCP}$) employed here in addition to the multipolar expansion of the $V_{\rm S}$, naturally play a very important role in describing the low-energy scattering behavior of the positrons. The matching between the $V_{\rm corr}^{\rm DFT}$ and the $V_{\rm pol}$ of Eq. (2) was done by locating on each C atom a ''polarizable center'' with a dipole polarizability value equal to 1/60 of the total polarizability of C_{60} and then by treating the resulting $V_{\rm pol}$ as the sum of 60 equal contributions for the different centers which can be once more described via the SCE form as used to represent the $V_{\rm S}$ and $V_{\rm corr}^{\rm DFT}$ potentials. This type of modeling, therefore, introduces a full nonspherical modeling of all the components of the $V_{\rm tot}$ interaction given in Eq. (4).

A further aspect of the calculations which should be mentioned at this point is the level of convergence which has been achieved in the partial-wave expansions of both the static potential and the scattering wave functions. While in the former case the level is controlled by the correct descrip-

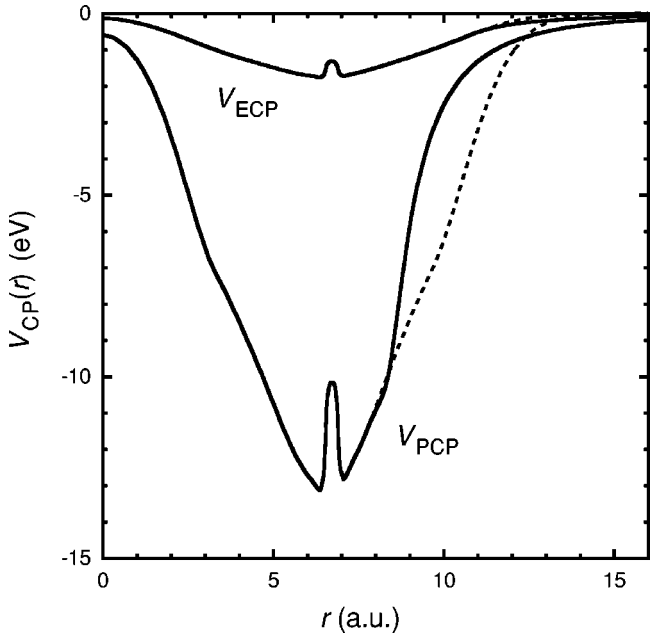

FIG. 1. Comparison of the spherically symmetric components of the computed V_{CP} model potentials employed in this work. See the main text for meaning of acronyms. The dashed lines correspond to the V_{corr} potentials, and the solid lines to the full V_{CP} potentials.

tion of the nuclear terms off the center of expansion, the latter depends on the number of coupled equations employed when solving Eq. (5). The *K*-matrix elements in the body-fixed frame were obtained by using a partial-wave expansions of the target wave function and of the scattered-positron continuum function with $l_{max}=40$. The interaction potential included the Coulomb and nuclear contributions to V_S up to $2l_{max}$. The expansion of the V_{CP} interaction was however truncated at $l_{max}=40$. The number of coupled equations, depending on the IR considered, varied from 9 in the a_u IR up to 77 for the h_g IR. The summed, partial contributions to both ICS's and DCS's included the a_g, a_u, t_{1g}, t_{1u}, t_{2g}, t_{2u}, g_g, g_u, h_g, and h_u components of the I_h point group. We have tested the stability of the final cross sections and found that they are converged to within 5–10 % with respect to increasing l_{max}. Another convergence parameter is maximum l included in the *K* matrix, which in the present study was $l_p=30$. With this truncation of the *K* matrix the total cross section is converged to within 0.01% with respect to increasing the size of the *K* matrix. We also note that this expansion of the *K* matrix yields differential cross sections which are converged to within approximately 1%.

In order to test computationally different V_{CP} model potentials, we have employed the formulation of Perdew and Zunger [23] for the V_{ECP} potential and the modified PCP2 potential of Jain [24] for the V_{PCP} as discussed above. A comparison of the spherical components for the two potentials is shown in Fig. 1, where we clearly see the much weaker nature of the V_{ECP} potential and the much stronger values of the V_{PCP} in the inner region of the interaction. We can also see in Fig. 1 how both of these potentials are connected to the asymptotic form of V_{CP} as described by Eq. (2).

Figure 2 reports the computational results which employed the V_{ECP} modeling of the V_{CP} interaction discussed above. The upper part shows the total, elastic integral cross

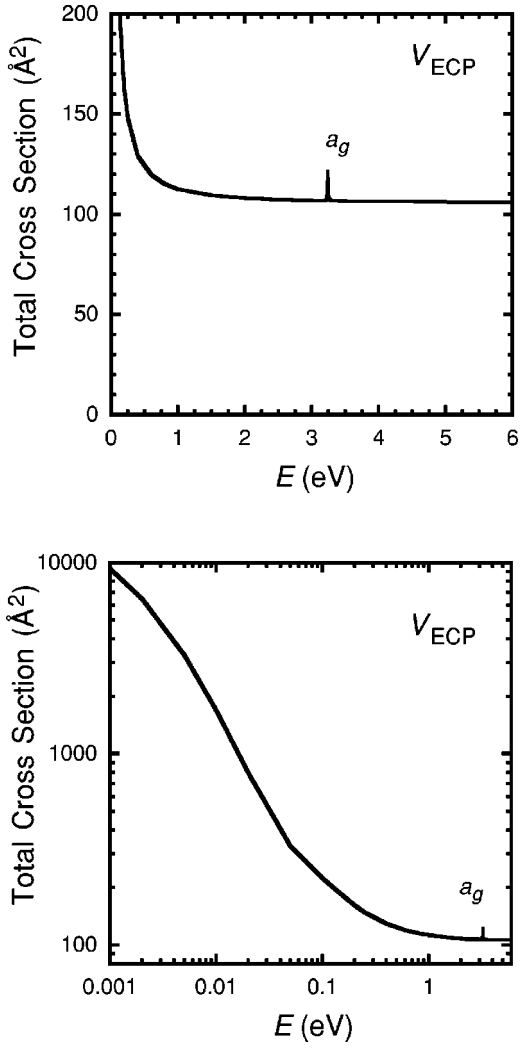

FIG. 2. Computed total, elastic ICS for positron scattering from C_{60} using the V_{ECP} in Eq. (4). Top panel: energy dependence of the ICS on a linear scale up to 6 eV. Bottom panel: same ICS energy dependence but on a log scale and down to 10^{-3} eV. All values of cross sections are in Å^2.

sections on a linear energy scale and up to 6 eV, i.e., above the expected threshold for Ps formation but still close enough to it that the elastic component is expected to have a dominant role. The lower panel of the same figure shows the same ICS calculations on a logarithmic scale. We note the following.

(1) As observed in many molecular systems, the ICS shows a marked increase as the collision energy decreases. This is chiefly due to the dominance of the long-range V_{pol} interaction for a nonpolar target like C_{60}. Hence, because of the presence of such a large polarizability, one sees that the cross section tends to a very large finite value (see lower panel of Fig. 2) and, below about 0.1 eV, becomes enormous, much larger than in any other measured system thus far: for the benzene molecule, for instance, the ICS values below the same energy are only about 30 Å^2 [31].

(2) For collision energies around 1 eV and above the present calculations show a very flat behavior of the ICS, as also surmised by the behavior of other molecular systems below Ps formation [32]. However, the present molecule is again quite unique in terms of the average size of such an

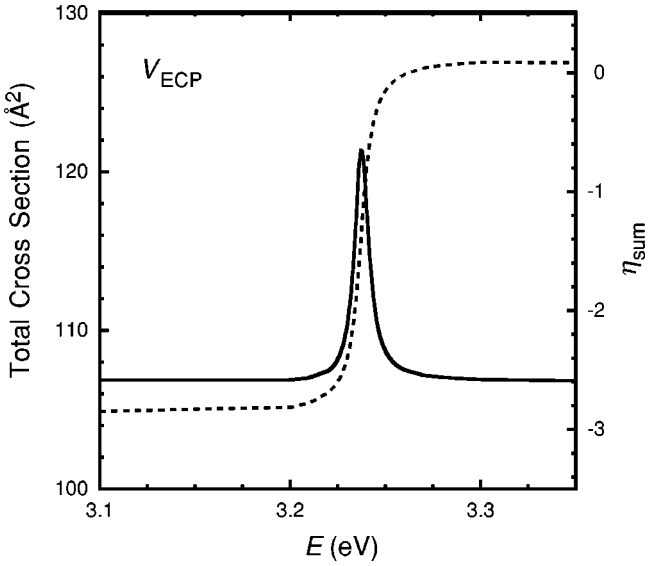

FIG. 3. Scattering cross sections and eigenphase sums at energies near the energy of the resonance of Fig. 2: solid line, computed total ICS (rotationally summed); dashed line, eigenphase sum η_{sum} for the dominant a_g contribution to the resonance.

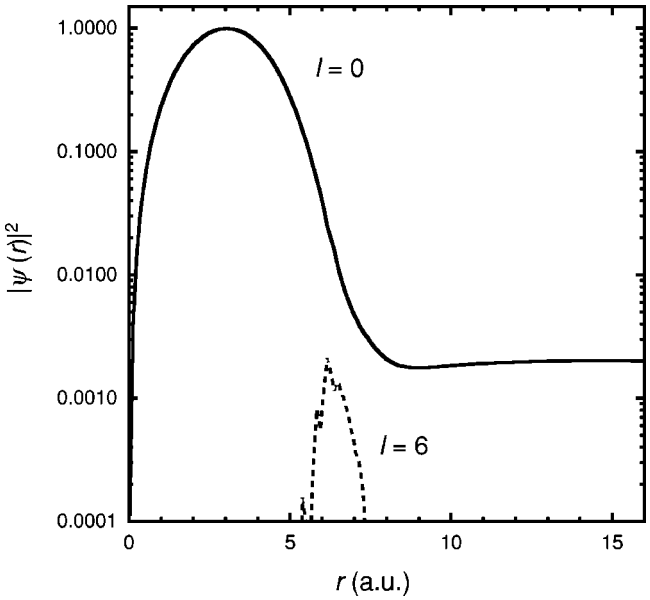

FIG. 4. Absolute square of the most important radial functions of the wave function of the a_g resonance at an energy of 3.238 eV and a width of 0.0088 eV obtained with the V_{ECP} potential.

ICS: the values remain around 100 Å^2, as opposed to average values of 10 Å^2 for the most common diatomics or small polyatomics [33,34].

(3) At the collision energy around 3 eV one clearly sees the presence of a well-marked resonance feature: a narrow peak in the ICS over a very limited energy range. The existence of fairly broad features in a similar energy region (around 2 eV) has been observed experimentally for several polyatomic molecules [33] and attributed there, albeit very qualitatively, to some form of open channel resonance. We believe this is the first instance in which calculations have shown such resonant features for positron-molecule scattering, as we shall discuss further below.

To analyze this feature better, in Fig. 3 we report further calculations of the ICS values in the peak region over a very narrow energy range. One clearly sees there that the shape of the resonance is quite distinct and that the enhancement has a peak value which is more than 10% above the background. To look at additional properties of the resonance, we have shown the behavior of the eigenphase sum for the a_g symmetry component, the only one which carries a resonant contribution to the total ICS at this low collision energy. The presence of an open-channel shape resonance can be detected very clearly as the η_{sum} increases by π radians across the resonance located at 3.238 eV. Its corresponding Wigner width turns out to be very small, i.e., only 8.8 meV, suggesting that such a resonance is unusually long lived and corresponds to the trapping of the positron behind a barrier for a very long time interval before decay ($\sim$0.5 ps).

In Fig. 4 we present the resonant wave function of the a_g resonance obtained with the V_{ECP} potential. One can see that the $l=0$ partial wave is dominant and that the state is trapped inside the C_{60} cage, which is located at $r=6.7$ a. u. In Fig. 5 we give the form of the $l=0$ radial effective adiabatic potential for the V_{ECP} and V_{PCP} potentials. We can see that both potentials are very repulsive at the location of the C_{60} cage due to the repulsive interaction of the positron with the C nuclei. This electrostatic repulsive potential is then able to trap the a_g resonant state in the V_{ECP} calculation.

Resonances in single-particle, open-channel cases have been known for electron scattering off molecules for a long time, and have been the subject of both theoretical and experimental studies for quite a while. Contrary to that situation, however, very little is known about resonances for positron scattering, in spite of their early prediction by the simple considerations of Massey [34]. Notwithstanding sev-

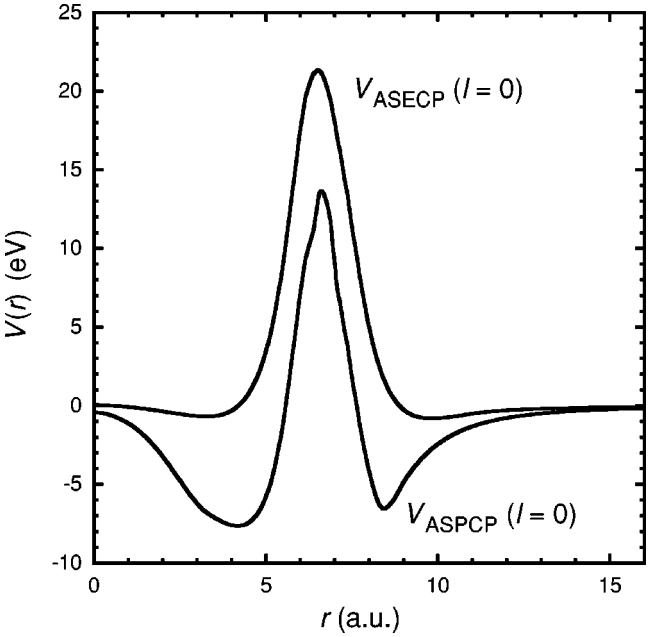

FIG. 5. Shape of the $l=0$ symmetry component of the V_{ASECP} and V_{ASPCP} interaction potentials. The C_{60} carbon cage is located at $r=6.7$ a. u., $r=0$ a. u. corresponds to the molecular center of mass.

eral experimental attempts based on positron annihilation detection, in fact, their existence has been still only surmised by circumstantial evidence. Although it is reasonable to expect that annihilation processes should affect the size and energy dependence even of elastic cross sections, very little information, either theoretical or experimental, exists on how much this is present in the low-energy collision processes.

Because of the chiefly repulsive nature of positron interaction with atoms and molecules, in fact, the attractive tail of the long-range $V_{\rm pol}$ usually creates fairly shallow wells located rather far outside the molecular charge distributions [35–37]. As a consequence of this feature, the additional presence of a centrifugal barrier tends to cancel the attraction, thus preventing shape resonances from appearing. On the other hand, in systems like C_{60}, the existence of a cage structure of nuclei and electrons away from the center of mass and over a rather large region of physical space, the corresponding presence of a very large dipole polarizability in the long-range $V_{\rm pol}$ and the absence of nuclear charges at the cage center, could lead to an overall interaction which is strongly ''shaped'' by a marked barrier which appears for $l=0$ potential. Furthermore, one can also expect that the additional presence of $l\neq 0$ barrier may be able in this system to produce pseudobound states at fairly low collision energies for other symmetries, as we shall discuss below.

Additionally in Fig. 5, one clearly sees the shape of the barrier just before the shallow attractive well outside of the C_{60} cage. As the energy increases the barrier becomes narrower and tunneling through it is likely to become more rapid, thereby broadening the resonance features. On the other hand, at the lower collision energy the barrier is wider and can more easily support pseudobound states with significant effects on both cross-section enhancement and decay-time delay across the bottom of the barrier.

It is worth pointing out here the rather special nature of the potential shown in Fig. 5, where the absence of nuclear repulsion effects at the core of the cage is the main cause of the inner potential well at such low energies, where the bottom of it follows closely the zero-energy baseline. In a similar, but smaller, system like benzene, for instance, the corresponding potential exhibits a small barrier at about 2.5 a. u. from the center of mass [38], but the baseline is about 6 eV above zero energy and its lowest pseudobound state appears around 41 eV, i.e., at much higher energy.

Thus, the unique spatial features of the C_{60} molecule are responsible for the correspondingly unique features of its $V_{\rm tot}$ potential, which suggests the presence of a long-lived open-channel resonance in the elastic cross section and at very low collision energy where detection would be more likely to occur [33].

A further indicator of the special nature of the ICS feature at 3.238 eV can be obtained by evaluating the total differential cross sections at that very energy, and by observing its behavior with respect to the same cross sections at another energy value. We have therefore carried out such calculations for all the IR's which contribute to the total, elastic DCS's for positron scattering from C_{60}. The results are shown in Fig. 6, where we indicate the DCS behavior at the energy of the resonance (the solid line) and the DCS shape at a nearby collision energy where no resonant effects are seen (the dashed line). The energy value chosen here was 4.0 eV.

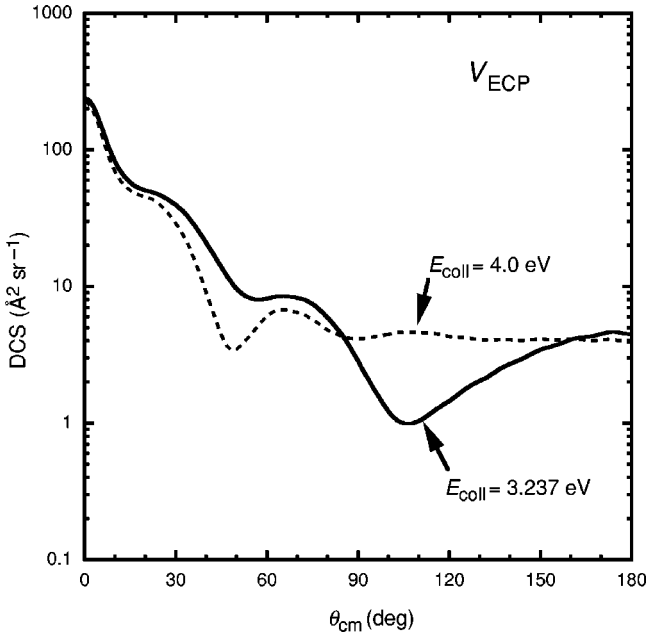

FIG. 6. Computed differential cross sections at collision energy values at and near the resonance presented in Fig. 3.

One clearly sees that, in spite of the dominance of the forward scattering behavior of positron dynamics, the resonant cross sections do show a marked peak in the large-angle region of the scattering.

As we mentioned earlier, the modeling of the $V_{\rm CP}$ interaction which is required to complete the description of the full potential of Eq. (4) can also be carried out by considering a positron projectile as an impurity within an electronic density provided by an electron gas, but represented here by our SCF computed electronic density of the bound electrons of the target [22,36]. In Figs. 1 and 5 we show that such a potential, $V_{\rm PCP}$, is markedly stronger than the $V_{\rm ECP}$ potential. Figure 7 reports the behavior of the total integral cross sections (over the same range of energies of Fig. 2) computed using the $V_{\rm PCP}$ for modeling the correlation-polarization effects. We clearly see the following.

(1) The corresponding elastic ICS's are now markedly larger and reach an average value of nearly 500 Å^2 above 1 eV. Clearly at low energy the polarization contributions dominate and the $V_{\rm PCP}$, because of its form, includes $V_{\rm corr}$ contributions which cross with the $V_{\rm pol}$ closer to the target than in the case of the $V_{\rm ECP}$ models (see Fig. 1).

(2) The *s*-wave, a_g resonance is now pushed down into the region of the bound states (positron trapping by formation of C_{60}^{+} molecules), while new resonances appear in the same low-energy region and for symmetries where centrifugal barriers are also present.

(3) The stronger potential causes the appearance of a t_{1u} resonance at 0.02 eV, of t_{2u} and g_u resonances at 0.5 eV, of g_g and h_g resonances at 1.5 eV, and a weak h_g resonance at 3.8 eV.

To analyze the resonances in the $V_{\rm PCP}$ calculation further, in Fig. 8 we give the effective radial potentials for the $V_{\rm ASPCP}$ potential. One can see both the electrostatic barrier at $r=6.7$ a.u. for all partial waves considered here and angular momentum barriers outside the C_{60} cage for the $l\geqslant 2$ radial potentials. In Fig. 9 we give the wave function for the reso-

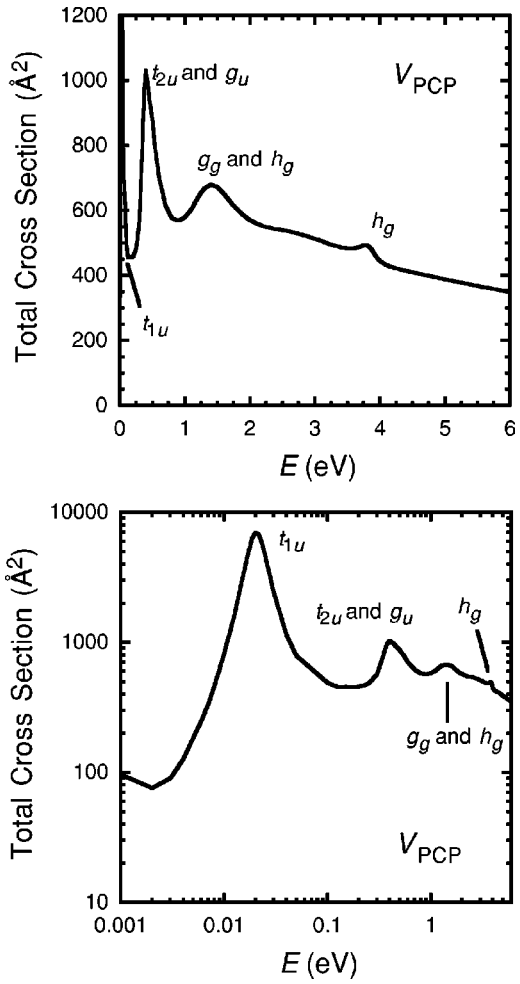

FIG. 7. Computed total ICS using the V_{PCP} potential discussed in the main text. The symmetry and positions of the various metastable cations are indicated by line segments and by their corresponding IRs.

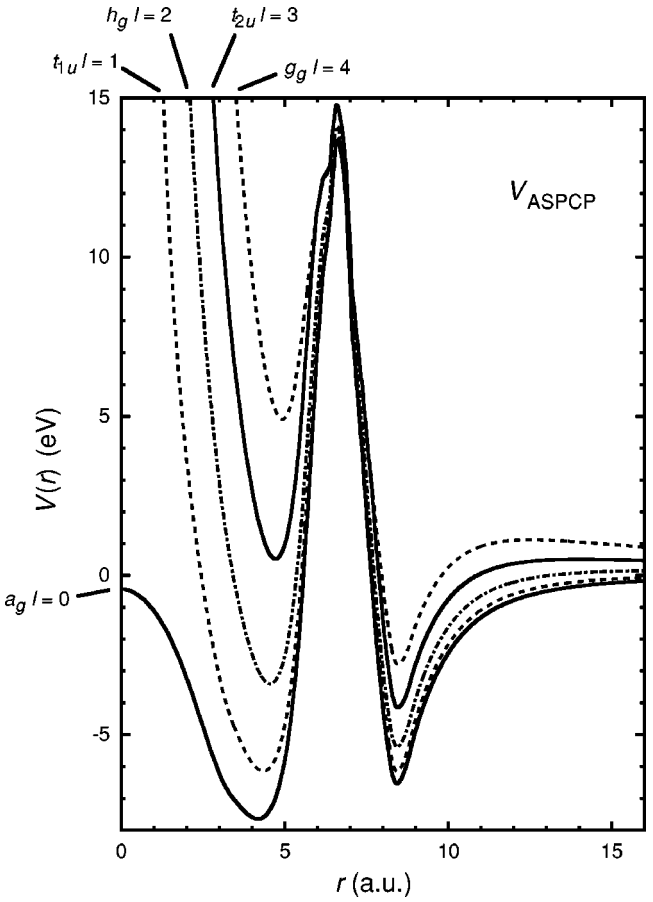

FIG. 8. The effective radial potentials of the V_{ASPCP} potential.

nance of h_g symmetry which occurs at 3.84 eV. We can see that this is a state which is predominately $l=2$ that is trapped inside of the C_{60} cage. In Fig. 10 we give the corresponding radial functions for the t_{2u} resonance which occurs at 0.47 eV. The probability density of this state is mostly outside of the C_{60} cage in the $l=3$ partial wave, and thus this state must be trapped by the $l=3$ angular-momentum barrier. The analysis of the other resonances leads to the following results: the t_{1u} resonance at 0.2 eV is an $l=1$ resonance trapped inside the cage; the t_{2u} resonance at 0.5 eV is an $l=3$ resonance trapped outside of the cage and behind the $l=3$ angular momentum barrier; the g_g and h_g resonances at $\sim$1.5 eV are $l=4$ resonances trapped outside of the cage by the $l=4$ angular-momentum barrier.

The effect of these resonances in the scattering using the V_{PCP} potential on the DCS is examined in Fig. 11, where we give the elastic DCS at an energy in the region of the t_{2u} and g_u resonances at 0.5 eV and at another energy of 3.0 eV, where there is no distinct resonance feature in Fig. 7. One can see the strong backward scattering in the region of the resonance with two minima which is characteristic of an $l=3$ resonant state. On the other hand, at the nonresonant energy there is mainly the expected strong forward scattering. The oscillatory nature of the 3.0-eV DCS is a result of the additional broad resonance of h_u symmetry which is predominantly an $l=5$ state trapped behind the $l=5$ angular momentum barrier. This angular-momentum assignment is in agreement with the number of peaks in the DCS seen at 3.0 eV.

One therefore sees that, contrary to what happens in other

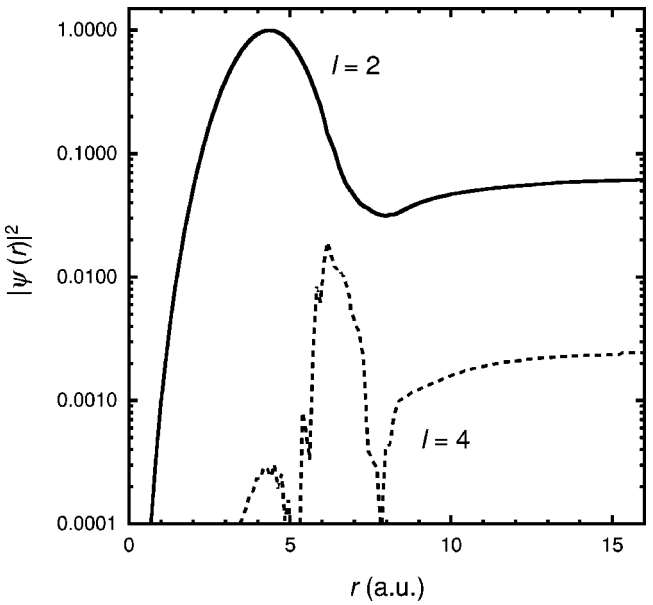

FIG. 9. Absolute square of the most important radial functions of the wave function of the h_g resonance at an energy of 3.84 eV and a width of 0.31 eV obtained with the V_{PCP} potential.

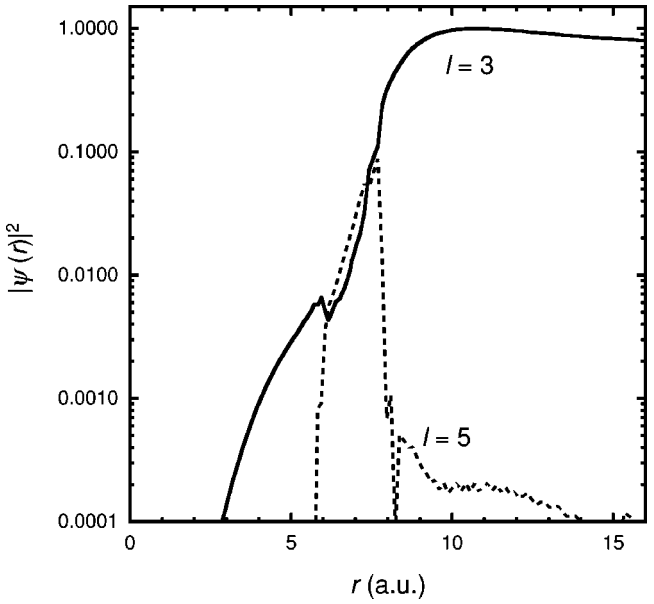

FIG. 10. Absolute square of the most important radial functions of the wave function of the t_{2u} resonance at an energy of 0.47 eV and a width of 0.20 eV obtained with the V_{PCP} potential.

molecular systems for which positron scattering can be computed, the existence of both very large values of the static dipole polarizability of the target and of the unusual spatial cage of the carbon atoms in the C_{60} molecule suggest strongly the possibility of low-energy positron trapping either inside the cage as in the V_{ECP} and V_{PCP} calculations or by the angular momentum barrier outside of the cage as found with the V_{PCP} potential. As a comparison, smaller but highly polarizable systems like CF_4 and CCl_4 show also very large values of ICS cross sections [39], but give no indication whatsoever of potential barriers which can support metastable states in the low-energy regions: as discussed before, their strong repulsive nuclear contributions to V_s prevent the occurrence of the specific potential ''shapes'' seen in the present system (Figs. 5 and 8).

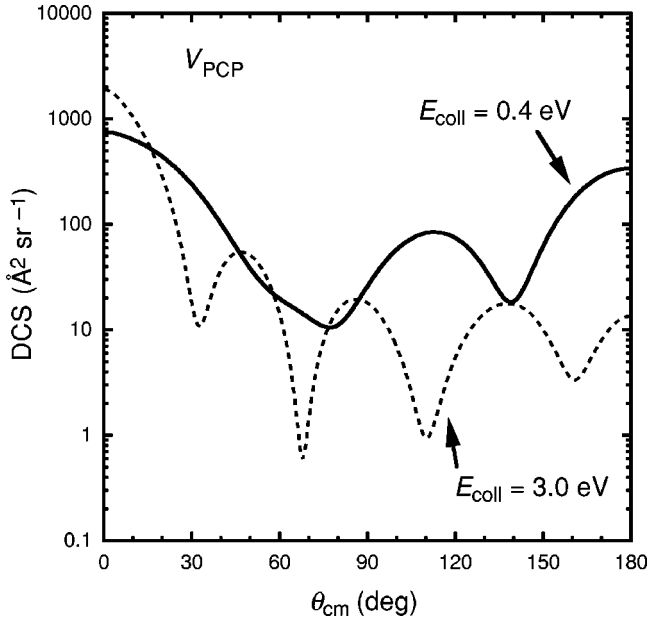

FIG. 11. Computed differential cross sections at the energy of the t_{2u} and g_u resonances seen in Fig. 7 (0.4 eV) and at an energy where there is no structure in the ICS (3.0 eV).

IV. CONCLUSION

We have carried out a computational study on the low-energy behavior for the total elastic ICS's for positron scattering from C_{60} in the gas phase. We believe this is the first time that the interaction of positrons with such a large molecular species has been considered and, to our knowledge, no previous results exist, either experimental or theoretical, for this dynamical process.

The calculations have found a series of features in the cross sections which are both in keeping with what should be expected and unusual in terms of some of their properties. In particular, the following chief points could be readily made and explained from what we have found in our study.

(1) The very large polarizability of the target appears to control the overall behavior of the integral cross sections, especially within a theoretical treatment which initially disregards the coupling with nuclear dynamics or with other degrees of freedom of the target.

(2) From collision energies of about 2 eV, and up to about 6 eV, the calculations show that the positron C_{60} cross sections could be much larger in size than those exhibited by electron scattering from the same molecule [40]. The increase in size for the cross sections in the case of either polar or highly polarizable molecules is in keeping with what has been found before for such systems [33], and indicates once more that for polyatomic targets with many degrees of freedom, this similarity, to be expected experimentally, can be confirmed by model calculations such as those carried out here.

(3) As the collision energy decreases below 2 eV, the calculations with the V_{ECP} potential show for the system an increase of the magnitude of the cross sections which rapidly tend to large finite values as E_{coll} goes to zero. This is also in keeping with what the experimental data have shown for many polyatomic molecules like benzene, hexane, cyclohexane, etc. [32,33]. Many of the measurements, in fact, indicate that the positron scattering cross sections become increasingly larger than the electron scattering cross sections as the collision energy goes below a certain threshold (usually around 3 eV). Here again the calculations show that our present models are capable of producing such a result in keeping with expected findings for large, highly polarizable targets.

(4) Depending on the V_{CP} potential used we see resonances either trapped inside of the C_{60} cage by the repulsive electrostatic potential or trapped outside of the cage by angular-momentum barriers. The existence of the resonances with the positron trapped inside the cage seems fairly certain, with the energy and symmetry being dependent on the strength of the attractive correlation potential. The states trapped outside of the cage will only be present if the correlation potential is fairly strong as is the case with the V_{PCP} potential.

(5) We have also studied the corresponding electron-C_{60} scattering system [41,40,42]. In electron scattering from C_{60} the FN cross sections exhibit a highly structured energy

dependence [40,42], with several peaks of varying widths due to a series of metastable one-electron shape resonances in the low energy regime. In contrast to electron scattering, positron scattering from the same target shows in our calculations a smoother behavior of the ICS over the same energy region, while further suggesting the appearance of a few possible resonances located around 3 eV and below (see Figs. 2 and 7). The mechanism for the formation of the resonances is somewhat different for the electron and positron scattering. In electron scattering there are in general only very low electrostatic barriers and the only mechanism for trapping is dynamical, i.e., the trapping is due to angular momentum barriers [27]. In e-C_{60} scattering the scattering resonances are all characterized by angular-momentum barriers with a major component of the scattered wave having $l \geqslant 7$ [42]. In positron scattering there are electrostatic barriers which can trap low-angular-momentum states of the positron inside of the C_{60} cage which we found in this study for $l \leqslant 2$. We also found angular-momentum trapped resonances in the positron scattering due to the strongly attractive polarization potential in the V_{PCP} case. When compared to the electron-molecule interaction, the the attractive part of the positron-molecule interaction is very weak; thus we again find only low-angular-momentum states dynamically trapped in positron-C_{60} scattering compared to the high-angular-momentum states in the electron scattering.

It is also worth mentioning at this point that, as a general rule, the peaks that appear in the total cross sections due to Ps formation tend to become weaker or less apparent as the size of the target molecule (or the number of the bound electrons) increases [33]. This is usually understood by a process of ''positron attachment,'' whereby a large number of electrons surrounds the impinging positron to form a quasistable ''bubble state'' within the molecular volume. The excess energy arising from the sum of the particle kinetic energy and the molecular positron affinity can then be efficiently distributed among the many molecular internal degrees of freedom which become rapidly more available in the larger molecular system [33]. In the present instance such considerations may suggest that, although located above the Ps formation threshold (but below the first electronic excitation threshold of C_{60}), the feature we are discussing could survive inclusion of nuclear degrees of freedom, and could also be detectable as a resonant feature, separate from possible interference with Ps formation channels that are deemed to be rather small for the present system at that energy. Eventually, of course, the trapped positron will either escape through the tunneling, leaving a neutral molecule, or annihilate by emitting a gamma ray and leaving behind a positive molecular ion. Thus, the existence of positron trapping during the scattering of slow positrons from gaseous C_{60} may be amenable to experimental observation either as an enhancement in the ICS, or as a structure in the angular distributions or, possibly, via the detection of rather stable molecular ions in their ground electronic states.

In any event, the present model calculations indicate rather clearly that positron scattering from such large molecular aggregates can lead to observations of the expected processes which, thus far, have only been suggested but not firmly established from positron scattering off smaller polyatomic aggregates in the gas phase. Some unique qualities of C_{60} (i.e., the large polarizability value and the extended distribution in space as a ''closed,'' cagelike structure) makes it one of the most likely candidates for finally being able to observe either positron metastable attachment to molecular aggregates (shape resonances) or positron bonding to a molecular structure via strong coupling between the resonant state and the internal degrees of freedom of C_{60} that would allow efficient energy dissipation, successfully competing with the direct tunneling of the resonant decay channel.

One open question, which the present calculations have further underlined, is a realistic treatment of short-range electron-positron correlation effects. Our model choices clearly indicate the strong dependence of results on the strength of the V_{CP} interaction. Similar calculations [39] on CF_4 and CCl_4 indicate that the true answer may be between the models which we have employed in the present study. However, the unique properties of C_{60} as a molecular target are clearly shown by either V_{CP} we used here, and should be confirmed by any other estimates of correlation effects.

A last caveat about the possible experimental detection of resonances as found in the present work may come from the possible effects of Z_{eff} values at the low energies. If such quantities were to be found rather large, as one might expect from the behavior of other large polyatomics, then they may give rise to additional resonant features. However, as none have been detected as explicitly related to annihilation processes, only future experimental data can help us to clarify this point.

ACKNOWLEDGMENTS

We are grateful to the NATO Scientific Division for the award of Collaborative Research Grant No. CRG950552, 922/94/JARC501. We also acknowledge the financial support of the Italian National Research Council (CNR) and the University of Rome Research Committee. One of us (R.R. L.) also wishes to thank the Welch Foundation (Houston) for its financial support under Grant No. A-1020 and to acknowledge the support of the Texas A&M University Supercomputing Facility.

[1] H. J. Ache, *Positronium and Muonium Chemistry* (Am. Chem. Soc. Press, Washington, DC, 1979).
[2] A. Passner, C. M. Surko, M. Leventhal, and A. P. Mills, Jr., Phys. Rev. A **39**, 3706 (1989).
[3] K. Iwata, R. G. Greaves, T. J. Murphy, M. D. Tinkle, and C. M. Surko, Phys. Rev. A **51**, 473 (1995).
[4] W. E. Kauppila and T. S. Stein, Adv. At., Mol., Opt. Phys. **26**, 1 (1989).
[5] K. Iwata, R. G. Greaves, and C. M. Surko, Phys. Rev. A **55**, 3586 (1997).
[6] G. Danby and J. Tennyson, J. Phys. B **24**, 3517 (1991).
[7] L. G. Christophorou, J. K. Olthoff, and M. V. V. S. Rao, J. Phys. Chem. Ref. Data **25**, 1341 (1996).
[8] D. Smith and P. Spanel, Adv. At., Mol., Opt. Phys. **32**, 307

(1994).
[9] S. Matejcik, T. D. Mark, P. Spanel, D. Smith, T. Jaffke, and E. Illenberger, J. Chem. Phys. **102**, 2516 (1995).
[10] F. A. Gianturco and D. De Fazio, Phys. Rev. A **50**, 4819 (1994).
[11] F. A. Gianturco, A. Jain, and L. C. Pantano, J. Phys. B **20**, 571 (1987).
[12] T. L. Gibson, J. Phys. B **23**, 767 (1990).
[13] See, e.g., E. A. G. Armour, Phys. Rep. **169**, 1 (1988).
[14] R. N. Hewitt, C. J. Noble, and B. H. Bransden, J. Phys. B **25**, 557 (1992).
[15] M. A. Morrison, Adv. At. Mol. Phys. **24**, 51 (1988).
[16] F. A. Gianturco, A. Jain, and J. A. Rodriguez-Ruiz, Phys. Rev. A **48**, 4321 (1993).
[17] F. A. Gianturco and J. A. Rodriguez-Ruiz, Phys. Rev. A **47**, 1075 (1993).
[18] F. A. Gianturco and R. Melissa, Europhys. Lett. **33**, 661 (1996).
[19] H. D. Meyer, Phys. Rev. A **40**, 5605 (1989).
[20] F. A. Gianturco, J. A. Rodriguez-Ruiz, and N. Sanna, Phys. Rev. A **52**, 1257 (1995).
[21] J. K. O'Connell and N. F. Lane, Phys. Rev. A **27**, 1893 (1983).
[22] E. Boronski and R. M. Nieminen, Phys. Rev. B **34**, 3820 (1986).
[23] J. P. Perdew and A. Zunger, Phys. Rev. B **23**, 5048 (1981).
[24] A. Jain, Phys. Rev. A **41**, 2437 (1990).
[25] F. A. Gianturco and A. Jain, Phys. Rep. **143**, 347 (1986).
[26] D. Fromme, G. Kruse, W. Raith, and G. Sinapius, Phys. Rev. Lett. **57**, 3031 (1986).
[27] R. R. Lucchese and F. A. Gianturco, Int. Rev. Phys. Chem. **15**, 429 (1996).
[28] F. A. Gianturco and R. R. Lucchese, J. Chem. Phys. **108**, 6144 (1998).
[29] M. J. Frisch, G. W. Trucks, H. B. Schlegel, P. M. W. Gill, B. G. Johnson, M. A. Robb, J. R. Cheeseman, T. Keith, G. A. Petersson, J. A. Montgomery, K. Raghavachari, M. A. Al-Laham, V. G. Zakrzewski, J. V. Ortiz, J. B. Foresman, J. Cioslowski, B. B. Stefanov, A. Nanayakkara, M. Challacombe, C. Y. Peng, P. Y. Ayal, W. Chen, M. W. Wong, J. L. Andres, E. S. Replogle, R. Gomperts, R. L. Martin, D. J. Fox, J. S. Binkley, D. J. Defrees, J. Baker, J. P. Stewart, M. Head-Gordon, C. Gonzalez, and J. A. Pople, *Gaussian 94* (Revision D.2) (Gaussian Inc., Pittsburg, PA, 1995).
[30] G. E. Scuseria, Chem. Phys. Lett. **176**, 423 (1991).
[31] M. R. Pederson and A. A. Quong, Phys. Rev. B **46**, 13 584 (1992).
[32] See, e.g., M. Kimura and H. Sato, Comments At. Mol. Phys. **26**, 333 (1991).
[33] M. Kimura, O. Sueoka, A. Hamado, and Y. Itikawa, Adv. Chem. Phys. (to be published).
[34] See, e.g., H. S. Massey, Phys. Today **29** (3), 42 (1976).
[35] F. A. Gianturco and P. Paioletti, Phys. Rev. A **55**, 3491 (1997).
[36] F. A. Gianturco and T. Mukherjee, Phys. Rev. A **55**, 1044 (1997).
[37] F. A. Gianturco, T. Mukherjee, and P. Paioletti, Phys. Rev. A **56**, 3638 (1997).
[38] F. A. Gianturco and R. R. Lucchese (unpublished).
[39] F. A. Gianturco, R. Curik, and N. Sanna (unpublished).
[40] F. A. Gianturco, R. R. Lucchese, and N. Sanna, J. Phys. B **32**, 2181 (1999).
[41] R. R. Lucchese, F. A. Gianturco, and N. Sanna, Chem. Phys. Lett. **305**, 413 (1999).
[42] F. A. Gianturco and R. R. Lucchese, J. Chem. Phys. **111**, 6769 (1999).